

Circulation beneath the Filchner Ice Shelf, Antarctica, and its sensitivity to changes in the oceanic environment: a case-study

K. GROSFELD, R. GERDES

Alfred-Wegener-Institut für Polar- und Meeresforschung, Postfach 120161, D-27515 Bremerhaven, Germany

ABSTRACT. We investigate the sensitivity of the ocean circulation in the Filchner Trough to changes in the large-scale oceanic environment and its impact on the mass balance of the Filchner Ice Shelf, Antarctica. Three experiments with a three-dimensional ocean model describe (i) the current situation, (ii) a scenario with increased ocean temperatures, and (iii) a scenario with reduced sea-ice formation rates on the adjacent continental shelf. In the final discussion brief results of a combined scenario with increased ocean temperatures and reduced sea-ice formation are presented. The changes from the current situation affect the circulation in the Filchner Trough, and melting and freezing processes beneath the ice shelf. The latter affect the amount and properties of Ice Shelf Water (ISW), a component of Antarctic Bottom Water. Net basal melt rates provide an overall measure for the changes: while the control run yields 0.35 m a^{-1} net melting averaged over the Filchner Ice Shelf area, the warming scenario results in a more than twofold increase in ice-shelf mass loss. Reduced production of High Salinity Shelf Water due to smaller sea-ice formation rates in the second scenario leads, on the other hand, to a decrease in basal mass loss, because the deep cavity is less well ventilated than in the control run. ISW is cooled and the ice shelf is stabilized under this scenario, which is arguably the more likely development in the southern Weddell Sea.

INTRODUCTION

Nearly half of the Antarctic shoreline consists of floating ice shelves. The mass balance of the ice shelves is determined by inflow from the land-based ice sheets, calving of icebergs at the ice-shelf edge, surface accumulation and melting, and mass exchange with the ocean at the ice-shelf base. All of these processes are likely to be affected by large-scale atmospheric and oceanic changes due to natural variability or anthropogenic changes. An atmospheric warming of 2.5°C during the last 50 years is the presumed cause of the disintegration of the northern Larsen Ice Shelf at the east coast of the Antarctic Peninsula (Vaughan and Doake, 1996). Another important factor is the access of warm waters, with respect to the in situ freezing point, to the ice-shelf cavity. This situation prevails along the Bellingshausen and Amundsen Seas east of the Antarctic Peninsula. Circumpolar Deep Water (CDW) of more than 1°C temperature that reaches the narrow continental shelf prevents the formation of large ice shelves and causes high basal melting (Hellmer and others, 1998). On the other hand, increased precipitation rates due to a gradual increase of atmospheric carbon dioxide, as in the coupled ocean–atmosphere model of Manabe and others (1992), can cause higher accumulation rates at the surface. Larger precipitation and the associated increase in stratification and in sea-ice cover can affect the ice shelf due to changes in water-mass formation and oceanic circulation. The interaction of ice shelf and ocean produces Ice Shelf Water (ISW), an important component of bottom water in the ocean (Foldvik and others, 1985a, b). To properly

estimate the sensitivity of the Antarctic ice sheet to climatic changes is therefore of major importance.

The Filchner–Ronne Ice Shelf in the southern Weddell Sea is the second largest ice shelf by area and the largest by volume. It comprises nearly $450\,000 \text{ km}^2$ (Fox and Cooper, 1994) and, together with the Ross Ice Shelf, drains the main part of the West Antarctic ice sheet and parts of the East Antarctic ice sheet. The Filchner Ice Shelf is the strongest source of ISW known in Antarctica (Gammelsrød and others, 1994) and therefore is an excellent area for studying the sensitivity to environmental changes of the ocean regime. Results for the Filchner Ice Shelf from two-dimensional thermohaline modelling (Hellmer and Olbers, 1991) showed a sensitivity of the circulation on both the salinity and the chosen flow path. Seasonal variability of source waters seems to modify the circulation and the depth and magnitude of ISW outflows. Nicholls (1997) has analyzed time series from moorings beneath the eastern Ronne Ice Shelf. The results of these measurements, namely, a reduced basal melt rate in summer, are in turn argued to be an analogue for a climate-warming scenario.

The circulation beneath ice shelves has been studied with a number of models of different complexity. Williams and others (1998) give a comprehensive overview of these modelling efforts. To simulate the response of the ocean–ice-shelf system to environmental changes a model must be general enough not to be constrained by parameterizations and assumptions that are tuned for current conditions and might not be valid under different climate regimes. Grosfeld and others (1997) introduced a three-dimensional model of the

ocean beneath an ice shelf and the adjacent open ocean that avoids additional assumptions on flow paths and conditions at the ice-shelf edge. While Grosfeld and others investigate the flow regimes for different idealized configurations, the model is here adapted for a realistic representation of the Filchner Trough beneath and in front of the Filchner Ice Shelf. We present results from a control run representative of recent conditions and from experiments that address two possible scenarios for a large-scale warming in Antarctica. The control run is integrated until a quasi-equilibrium is reached, and the experiments continue for 5 years from that state. The first experiment explores the access of warmer waters into the ice-shelf cavity, while the second considers a shut-down of High Salinity Shelf Water (HSSW) production on the shallow shelf north of Berkner Island. Both scenarios are possible, given the experience from climate models and recent observations of the disintegration of certain ice shelves.

MODEL SET-UP

The ocean model is described in detail by Grosfeld and others (1997). It uses the Boussinesq, hydrostatic and anelastic approximations. Horizontal velocity components, potential temperature and salinity are the prognostic variables. Density is calculated as a function of potential temperature, salinity and depth according to Mellor (1991). The model is formulated on an s -coordinate grid (Gerdes, 1993) where sea bottom and ice-shelf base are coordinate surfaces. Diffusion and friction are formulated as harmonic mixing along s -surfaces for tracers ($A_{HH} = 100 \text{ m}^2 \text{ s}^{-1}$) and momentum ($A_{MH} = 60 \text{ m}^2 \text{ s}^{-1}$). Vertical mixing coefficients are $A_{MV} = 10^{-3} \text{ m}^2 \text{ s}^{-1}$ for momentum and $A_{HV} = 5 \times 10^{-5} \text{ m}^2 \text{ s}^{-1}$ for tracers. A convective adjustment scheme removes hydrostatic instability within the water column.

The model is forced by an idealized wind-stress field, matched to European Centre for Medium-range Weather Forecasts annual mean conditions (Kottmeier and Sellmann, 1996). A simple diagnostic sea-ice model is used which estimates the heat flux across the sea surface from the difference between sea-surface temperature, fixed at the sea-surface freezing point, and the uppermost ocean layer. Atmospheric coupling and heat conduction through the ice is neglected. Melt and freeze rates and associated buoyancy fluxes for the ocean are calculated from latent-heat fluxes (for further details see Grosfeld and others (1997)). In the case of no sea ice, temperature and salinity of the ocean surface is restored towards -1.9°C and 34.4, respectively. Since the model includes neither an atmospherically forced seasonal cycle nor sea-ice transports, it cannot reproduce the formation of HSSW, which results from brine rejection due to strong sea-ice production during winter. This process is most effective in coastal polynyas that are due to offshore winds. A realistic representation of HSSW formation, therefore, needs a complex dynamic/thermodynamic sea-ice model which has not yet been coupled to our ocean model. Formation of HSSW is incorporated in our model in a parameterized form, according to observations and measurements. One major area of HSSW production is the shallow Berkner Bank, north of Berkner Island (Foldvik and others, 1985b; Schröder and others, 1997). South of $76^\circ 30' \text{ S}$, salinities are adjusted towards a profile increasing from 34.55 at the surface to

34.68 at the bottom, according to these measurements. Temperatures are restored towards a constant value of -1.9°C . The adjustment time-scale for both tracers is 30 days. The conditions south of Berkner Island are restored to salinities found in the model of Determann and others (1994) to prevent desalination due to melting in that area and to incorporate exchanges with the Ronne Ice Shelf cavity.

The circulation in the sub-ice-shelf cavity is forced by buoyancy fluxes across the interface between the cavity and the open ocean and by melting and freezing at the ice-shelf base. The freezing point of sea water depends on pressure and varies from -1.9°C at the ocean surface to about -2.7°C at 1000 m depth. The temperature difference between the cold ice-shelf base and the ambient ocean water drives the “ice-pump” mechanism (Lewis and Perkin, 1986). Cold waters are produced near the deep grounding line by melting of glacial ice. The subsequent rise along the ice-shelf base yields supercooled water, which releases ice crystals that accumulate at the ice-shelf base (Jenkins and Bombosch, 1995). This fresh-water extraction increases salinity and temperature in the ocean. In the model this process is parameterized in the form of a simple bulk formulation for the turbulent-heat exchange between the ice-shelf base and the adjacent ocean layer, following Determann and Gerdes (1994).

The model domain is limited to the west by a closed boundary along $47^\circ 30' \text{ W}$ and the coastline of Berkner Island, and to the east by the Coats Land coast. The model domain covers the Filchner Ice Shelf from 82° to $78^\circ 18' \text{ S}$ and extends up to the shelf break at about 75° S . The northern boundary of the model is closed. This allows us to prescribe boundary values (as in scenario (a) below) at the boundary without the need to simulate the changes in the open ocean explicitly. The closed boundary represents no restriction for the model results; the control run reproduces the main features of the recent regime in the Filchner Trough.

he domain is discretized onto a rectangular grid with grid distances of 0.1° in latitude and 0.3° in longitude. The vertical grid contains 10 s -layers in the cavity, varying from 24% of water-column thickness for the uppermost layers to about 25% for the bottom layer. Four additional layers of constant depth (40 m) are added in the upper part of the open ocean. These layers end at the ice-shelf edge. The data base for bedrock topography is taken from the digital Institut für Angewandte Geodäsie map (Vaughan and others, 1994); ice-shelf draft is derived from surface elevation data (Wingham and others, 1997) using hydrostatic arguments. The ice edge is chosen constant along $78^\circ 18' \text{ S}$, according to the situation after the calving of the three giant icebergs in 1986 (Ferrigno and Gould, 1987). Initially the potential temperature is -1.9°C in the open ocean and decreases by $0.1^\circ\text{C}/^\circ \text{ lat}$. south of the ice edge to avoid high melt rates during spin-up. Initial salinity is constant (34.60) on all levels. Integration starts from the ocean at rest and continues until a quasi-steady state is reached after about 10 years.

RESULTS

Control run

The stream function for the vertically integrated mass transport in the control run (Fig. 1) shows a cyclonic gyre in the trough in front of the ice shelf. The southward flow of about 1.6 Sv ($1 \text{ Sv} = 10^6 \text{ m}^3 \text{ s}^{-1}$) from the sill along the eastern flank

of the Filchner Trough brings water from the shelf break to the sub-ice-shelf cavity. The main gyre is located in the interior of the depression and increases to about 2.5 Sv, while the circulation on the shelves along Coats Land and in front of Berkner Island is less intense. A small sub-gyre (0.3 Sv) forms a weak westward flow on the northern Berkner Bank. Experiments with a domain including the open ocean beyond the shelf break show the same pattern of a gyre in the Filchner Depression with a small outflow across the sill at 32° W with a ratio of about 1:2 between the overflow and the recirculation in the depression. This value indicates good agreement between the gyre flow in the present model (~ 2 Sv in the northern Filchner Trough) and the transport measurements of 1 Sv in the overflow plume at the continental slope by Foldvik and others (1985a).

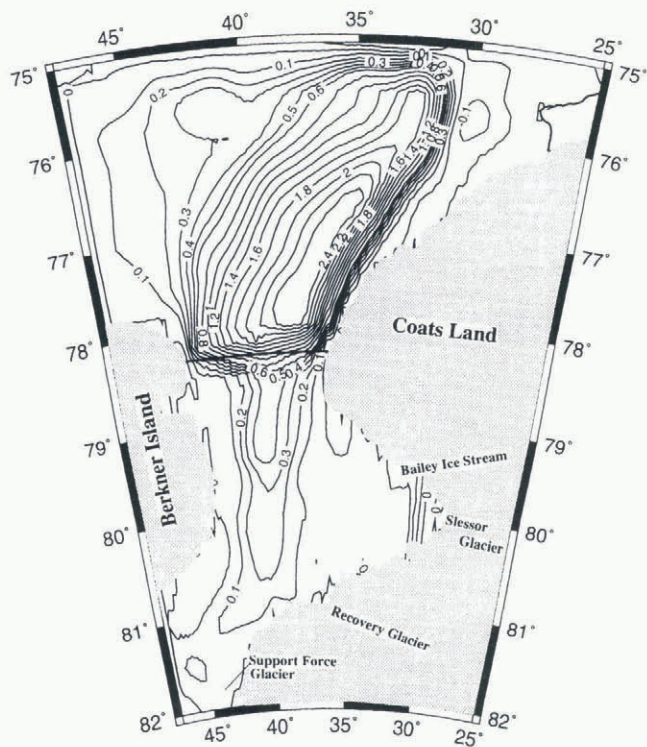


Fig. 1. Stream function for the vertically integrated mass transport (Sv) in the control run. The main gyre rotates in a clockwise fashion (cyclonic).

In front of the ice shelf at 78°18' S the vertically integrated flow abruptly turns westward due to the sudden decrease in water-column depth, which blocks barotropic flow across the ice edge (Grosfeld and others, 1997). About 0.4–0.6 Sv enters the cavity west of the steepest bottom slope, which is in good agreement with the estimates of Carmack and Foster (1975). Because of the 1200 m depth of the Filchner Trough in front of the ice edge, the reduction of the water-column thickness is only $\sim 40\%$. Hence, the barotropic flow is not as completely blocked as it has been found to be over large parts of the eastern Ronne Ice Shelf edge in other model experiments (Determann and others, 1994). The main gyre reaches south to about 80°30' S in the sub-ice-shelf cavity. The eastern part of the cavity is decoupled from the main circulation system beneath the ice shelf, because of the shallow water-column depths of 100–300 m, compared to about 600–800 m in the main trough.

A meridional transect along 41°30' W presents the hydrographic situation in the Filchner Trough as simulated

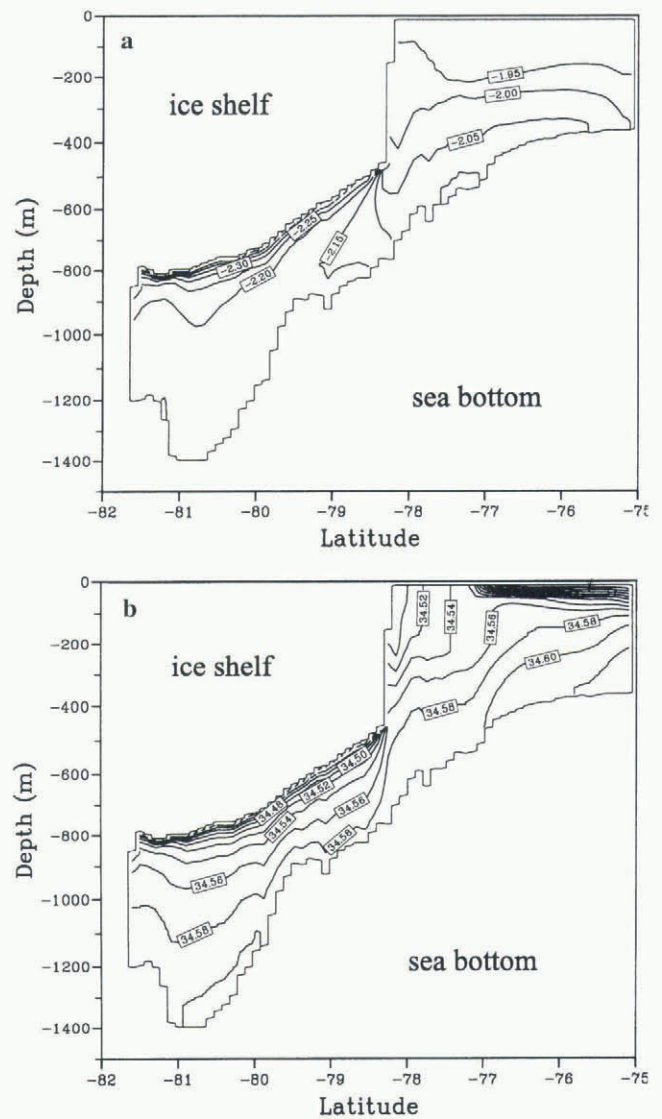


Fig. 2. (a) Potential temperature in °C, and (b) salinity along a meridional transect 41°30' W through the Filchner Trough for the control run.

by the model (Fig. 2). This transect contains both information from the inflowing water mass as it ventilates the cavity from the open ocean, and the impact of ice-shelf–ocean interaction (melting and freezing processes at the ice-shelf base) on the stratification in the cavity. The potential temperature distribution (Fig. 2a) shows a shallow thermocline in the deep part of the cavity with lowest temperatures of -2.52°C at the ice-shelf base. The lower part of the water column (-2.15° to -2.20°C) is less stratified. The temperature increases from south to north due to the admixture of inflowing warmer waters from the east. The ice-shelf cavity is depleted in salinity (Fig. 2b) due to melting of ice and the corresponding fresh-water gain. Near the ice edge, basal freezing and associated salt release destabilize the stratification. However, salinity does not reach its original value, because of net melting of ice over the ice-shelf area. The main outflow of ISW occurs between the bottom and intermediate depth, and is only partly included in a vertical ice pump, which rises up to the surface and causes strong sea-ice formation, evidenced by vertical homogeneity in the salinity distribution (Fig. 2b). Steered by the topography, ISW flows along the western flank of the trough, where it mixes with HSSW from the Berkner Bank. Further on (not shown), the water recirculates in the deep trough, where it

is enriched in salinity and temperature by entrainment, before it re-enters the deep cavity. The signal of the inflowing HSSW is clearly discernible in Figure 2 as the salinity maximum at the bottom near the northern boundary.

The interaction of the ocean with the ice-shelf base causes melting and freezing patterns which are an important factor in the mass balance of the ice shelf. Since the

Table 1. Melting and freezing rates for Filchner Ice Shelf under different oceanic conditions

	Central ice-shelf > 100 km		Edge area < 100 km		Total net basal mass loss m a ⁻¹
	Melting	Freezing	Melting	Freezing	
	Gt a ⁻¹	Gt a ⁻¹	Gt a ⁻¹	Gt a ⁻¹	
Control run	19.2	1.8	8.0	2.6	0.35
Scenario (a)	32.2	1.6	25.7	3.1	0.81
Scenario (b)	14.4	1.7	8.2	1.9	0.29
Scenario (c)	18.6	1.5	10.3	1.9	0.38

Notes: The total net basal mass loss is calculated over the ice-shelf area of 71 800 km² with an ice density of 917 kg m⁻³. Melting and freezing rates are calculated separately for the edge area (within 100 km of the ice-shelf edge) and the central ice shelf. Scenario (a) considers a temperature increase (+0.6°C) of the inflowing water. In scenario (b) the source of HSSW on the Berkner Bank is switched off. Scenario (c) combines (a) and (b) with increased inflowing temperatures (+0.1°C) and lack of HSSW production.

results of this ocean model are discussed in detail by Grosfeld and others (1998) with respect to marine ice formation beneath the ice shelf, we restrict ourselves to the net basal mass balance (Table 1). The interaction between the open ocean and the ice-shelf cavity is greatest in the seaward 100 km. Therefore, we distinguish in our calculation between the edge area (<100 km from the ice edge) and the central ice shelf. The calculated melt rate in the ice-edge area might be underestimated since tidal motions are not included in the model. Nevertheless, downwelling of surface waters as a consequence of Ekman pumping increases melting and thus water-mass exchange in the edge area. For the control run, 8.0 Gt a⁻¹ of melting and 2.6 Gt a⁻¹ of freezing in the coastal area, and 19.2 Gt a⁻¹ of melting and 1.8 Gt a⁻¹ of freezing in the central ice shelf have been estimated. This results in a mean net basal melt rate of 0.35 m a⁻¹ over the whole ice shelf. The high proportion of freezing in the edge area is perhaps surprising, as one would expect a strong melting zone along the whole ice-shelf edge, as discussed by Jacobs and others (1992). However, this result reflects the special situation of the Filchner Ice Shelf domain, where the deep trough between Berkner Island and Coats Land enables an almost closed horizontal circulation system rather than vertical overturning processes. This leads to a pattern with melting along the eastern part, the inflow of the main gyre, and freezing along the western part, the recirculation and outflowing branch of the gyre.

(a) Impact of warmer waters accessing the ice-shelf cavity

As stated in the introduction, flooding of warm waters onto continental-shelf regions and further south into the Filchner–Ronne Ice Shelf cavity is a potential source of increased erosion and destabilization of the ice shelf. To study this effect for the Filchner Ice Shelf cavity, we increase

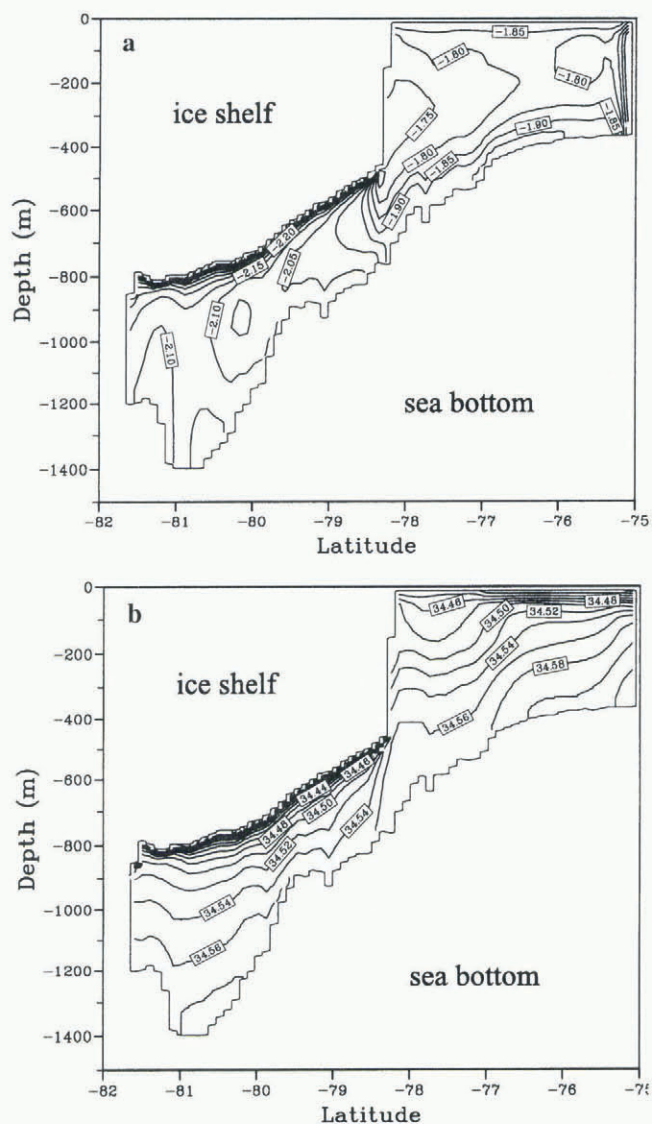


Fig. 3. (a) Potential temperature in °C, and (b) salinity along a meridional transect 41°30' W through the Filchner Trough for increased water temperatures in the open ocean (scenario (a)).

the temperature at the northern boundary of our model to simulate an increase in the temperature of Warm Deep Water (WDW), the Weddell Sea’s modified CDW. Since the width of the southern Weddell Sea continental shelf is a natural barrier to the direct access of WDW to the Filchner–Ronne Ice Shelf complex, only its derivative Modified Warm Deep Water (MWDW), a mixture of WDW and Winter Water, is able to penetrate further south. Whether warming of the Southern Ocean would lead to a similar increase in MWDW temperatures is unclear. We therefore fix the temperature to -1.3°C, the temperature of MWDW found on the southern Weddell Sea shelf (Schröder and others, 1997). This corresponds to a 0.6°C temperature increase of the accessing water mass in the model.

The main gyre in the central Filchner Trough decreases to about 1.8 Sv, while the circulation in the ice-shelf cavity remains nearly the same. The gyre spreads in the zonal direction. Potential temperature (Fig. 3a) and salinity (Fig. 3b) along 41°30' W depict the influence of the temperature increase. The deep cavity is ventilated with waters more than 0.05°C warmer than in the control run. Increased melting reduces the salinity of the outflow, and the Filchner Trough fills up with less saline and warmer ISW. The change

in ISW properties could influence the overflow at the continental sill, deep and bottom water formation in the Weddell Sea and eventually the global ocean.

In the deep cavity the mass loss due to melting increases to 32.2 Gt a^{-1} , while freezing is only 1.6 Gt a^{-1} . In the edge area, melting amounts to 25.7 Gt a^{-1} and freezing to 3.1 Gt a^{-1} . Although increasing in the edge area, freezing cannot compensate the dramatically increased overall melting. The calculated mean basal mass balance for the whole ice-shelf area is 0.81 m a^{-1} ; net melting in the central ice shelf is 0.61 m a^{-1} and in the edge area 1.45 m a^{-1} .

(b) Impact of reduced HSSW production

HSSW forms in the coastal polynya, and especially on the shallow continental shelf north of Berkner Island, due to brine rejection during wintertime sea-ice formation (Foldvik and others, 1985b). The control run shows this saline water mass ($S \geq 34.58$ in Fig. 2b) ventilating the ice-shelf cavity. Increased precipitation and less sea-ice production due to thicker ice cover, as in the gradual CO_2 -increase simulation of Manabe and others (1992), could suppress HSSW production. A compact ice cover insulates the ocean against the cold atmosphere and suppresses sea-ice formation and brine rejection.

Such a situation was recently observed in front of the Filchner Ice Shelf after calving of the giant icebergs in 1986. Due to the grounding of the icebergs on the shallow Berkner Bank, sea ice accumulated east of these icebergs instead of being advected further westwards. A fast ice tongue formed and the polynya in front of the Filchner ice edge did not occur. It has been observed (Schröder and others, 1997) that HSSW production in the Filchner Trough and over the Berkner Bank was reduced after this event. To investigate the influence of reduced HSSW production on the Berkner Bank, we switched off HSSW restoring for 5 years after a steady state was reached during the control run.

The vertically integrated mass transport decreases to $\sim 2.0 \text{ Sv}$ in the open-ocean part of the central depression and to $\sim 0.4 \text{ Sv}$ in the cavity. The gyre penetrates only to the shallower parts of the cavity. Correspondingly, the outflow of ISW reduces and the production of sea ice in front of the ice shelf due to upwelling ISW decreases. However, due to the reduced transport of waters at surface freezing-point temperature into the cavity, the temperature in the cavity decreases and an outflow of colder ISW can be observed (Fig. 4a). The deep trough fills up with ISW that is less saline because the flux of HSSW off the Berkner Bank into the depression disappears (Fig. 4b). The water in the deep cavity becomes colder and less saline. This leads to a reduced melting rate of 14.4 Gt a^{-1} , while freezing changes very little (1.7 Gt a^{-1}), and thus has stabilizing effect on the whole ice shelf. The resulting net basal melt rate for the whole ice shelf is 0.29 m a^{-1} , where 0.40 m a^{-1} of net melting occurs in the edge area and only 0.25 m a^{-1} in the central ice-shelf area. Nevertheless, outflow and upwelling of ISW continues, establishing a vertical ice pump which supplies sea-ice production in front of the ice shelf (Fig. 4b). This is evidenced in the vertical mixed-salinity profile with, however, clearly reduced salinity compared to the control run (Fig. 2b).

DISCUSSION AND CONCLUSION

We have applied a three-dimensional ocean model to the

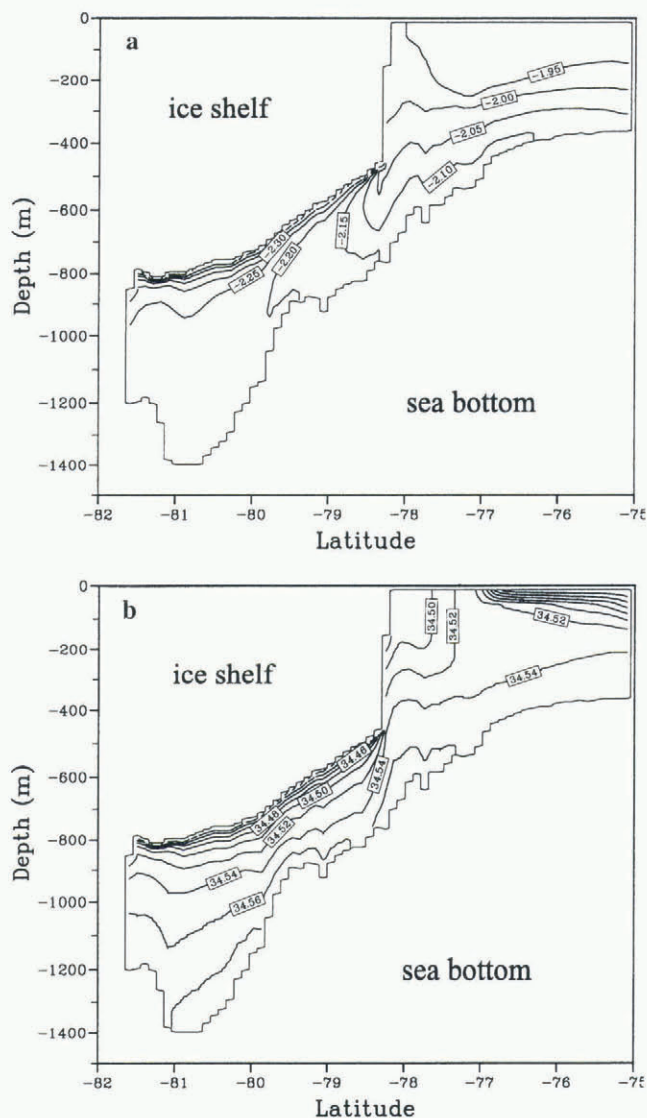


Fig. 4. (a) Potential temperature in $^{\circ}\text{C}$, and (b) salinity along a meridional transect $41^{\circ}30' \text{ W}$ through the Filchner Trough for reduced HSSW on Berkner Bank (scenario (b)).

Filchner Ice Shelf domain in the southern Weddell Sea to study the sensitivity of the ice-shelf–ocean system to changes in the oceanic environment. The control run which was designed to represent the recent situation in the Filchner Trough exhibits a cyclonic gyre in the deep trough in front of the ice shelf. A reduced flow of about $0.4\text{--}0.6 \text{ Sv}$ enters the cavity with southward inflow along the Coats Land coast and northward outflow along the east coast of Berkner Island. The circulation system features a mainly horizontal circulation instead of the often-discussed vertical overturning with deep inflow and shallow outflow in ice-shelf cavities. The calculated mean basal mass balance accounts for 0.35 m a^{-1} of melting over the whole ice shelf.

Two sensitivity studies were performed to investigate the response of the ice-shelf–ocean system to changed hydrographic conditions in the adjacent ocean. The warming scenario (a) depicts an expected increase in basal erosion due to the ventilation of the ice-shelf cavity with waters warmer than in the control run. Scenario (b) yields a different result: reducing or switching off the source of dense water on the Berkner Bank leads to a decreased ventilation of the deep ice-shelf cavity. The smaller heat transport into the

deep cavity reduces basal melting beneath the thick glaciers near the grounding line. Consequently, stabilization, rather than disintegration of the ice shelf is a possibility.

This result contrasts with the findings of MacAyeal (1984), who pointed out that ablation beneath ice shelves is less sensitive to climate changes, as the main driving water mass for the thermohaline circulation, the HSSW, is fixed at surface freezing point. Changes in production rate and pathways of HSSW were, however, not considered by MacAyeal. A similar result to ours has been obtained by Nicholls (1997) from mooring data beneath the Ronne Ice Shelf. He found that the seasonal reduction in HSSW production during summer yields thinner HSSW layers beneath the ice shelf and thus a smaller heat source for melting than during winter. Nicholls transferred his results to a climate-warming scenario and concludes that the initial response would be a thickening of ice shelves instead of their decline.

The dynamic response of an ice shelf to such a development is much more difficult to predict. Two time-scales have to be distinguished in the discussion of the impact of climate warming on the ice-shelf cavity circulation. From scenario (a) we can conclude that a general warming of accessing waters to an ice-shelf cavity will in any case lead to increased melting at the ice-shelf base and will therefore contribute to ice-shelf decline. This process comprises a long time-scale, because warming of MWDW is a result of the mixing of Winter Water and warmed WDW. The latter depends very much on changed sea-ice conditions in the Weddell Sea and the access of warmed CDW to the Weddell Gyre.

On shorter time-scales, however, climate warming might increase the sea-ice cover in the Weddell Sea, which yields reduced basal erosion of the ice shelf and has a stabilizing effect after scenario (b). Modification of MWDW within this time-scale is expected to be very small. A combination of both effects appears to be most realistic for a greenhouse warming scenario for medium time-scales. A model experiment with a moderate MWDW warming (0.1°C) and a simultaneous shut-down of HSSW production leads to a ~10% increase in the overall basal mass loss (Table 1, scenario (c)). Detailed analysis of the experiment shows that melting in the ice-edge area increases, while melting in the central ice-shelf area decreases, thus stabilizing the ice shelf.

Since the huge Filchner–Ronne and Ross Ice Shelves are sheltered from the direct access of CDW by wide and shallow shelf areas, the influence of climate warming on these areas is more likely to derive from a change in sea-ice conditions in front of the ice shelves than from warmer ocean temperatures. Reinforcement of the Filchner–Ronne Ice Shelf, rather than destabilization and eventual disintegration, is therefore the likely prospect for the near future.

ACKNOWLEDGEMENT

Travel funding by the Deutsche Forschungsgemeinschaft is gratefully acknowledged. This is contribution No. 1326 of the Alfred-Wegener-Institut für Polar- und Meeresforschung.

REFERENCES

- Carmack, E. C. and T. D. Foster. 1975. Circulation and distribution of oceanographic properties near the Filchner Ice Shelf. *Deep-Sea Res.*, **22**(2), 77–90.
- Determann, J. and R. Gerdes. 1994. Melting and freezing beneath ice

- shelves: implications from a three-dimensional ocean-circulation model. *Ann. Glaciol.*, **20**, 413–419.
- Determann, J., K. Grosfeld, R. Gerdes and H. Hinze. 1994. Melting and freezing rates beneath Filchner–Ronne Ice Shelf from a 3D-ocean circulation model. In Orter, H., ed. *Filchner–Ronne Ice Shelf Programme. Report 8*. Bremerhaven, Alfred Wegener Institute for Polar and Marine Research, 12–19.
- Ferrigno, J. G. and W. G. Gould. 1987. Substantial changes in the coastline of Antarctica revealed by satellite imagery. *Polar Rec.*, **23**(146), 577–583.
- Foldvik, A., T. Gammelsrød and T. Tørresen. 1985a. Circulation and water masses on the southern Weddell Sea shelf. In Jacobs, S.S., ed. *Oceanology of the Antarctic continental shelf*. Washington, DC, American Geophysical Union, 5–20. (Antarctic Research Series 43.)
- Foldvik, A., T. Gammelsrød, N. Slotsvik and T. Tørresen. 1985b. Oceanographic conditions on the Weddell Sea shelf during the German Antarctic Expedition 1979/80. *Polar Res.*, **3**(2), 209–226.
- Fox, A. J. and A. P. R. Cooper. 1994. Measured properties of the Antarctic ice sheet derived from the SCAR Antarctic digital database. *Polar Rec.*, **30**(174), 201–206.
- Gammelsrød, T. and 9 others. 1994. Distribution of water masses on the continental shelf in the southern Weddell Sea. In Johannessen, O. M., R. D. Muench and J. E. Overland, eds. *The polar oceans and their role in shaping the global environment: the Nansen Centennial volume*. Washington, DC, American Geophysical Union, 159–176. (Geophysical Monograph 85.)
- Gerdes, R. 1993. A primitive equation ocean circulation model using a general vertical coordinate transformation. I. Description and testing of the model. *J. Geophys. Res.*, **98**(C8), 14,683–14,701.
- Grosfeld, K., R. Gerdes and J. Determann. 1997. Thermohaline circulation and interaction between ice shelf cavities and the adjacent open ocean. *J. Geophys. Res.*, **102**(C7), 15,595–15,610.
- Grosfeld, K., H. H. Hellmer, M. Jonas, H. Sandhäger, M. Schulte and D. G. Vaughan. 1998. Marine ice beneath Filchner Ice Shelf: evidence from a multi-disciplinary approach. In Jacobs, S. S. and R. F. Weiss, eds. *Ocean, ice and atmosphere: interactions at the Antarctic continental margin*. Washington, DC, American Geophysical Union, 321–341. (Antarctic Research Series 75.)
- Hellmer, H. H. and D. J. Olbers. 1991. On the thermohaline circulation beneath the Filchner–Ronne Ice Shelves. *Antarct. Sci.*, **3**(4), 433–442.
- Hellmer, H. H., S. S. Jacobs and A. Jenkins. 1998. Oceanic erosion of a floating Antarctic glacier in the Amundsen Sea. In Jacobs, S. S. and R. F. Weiss, eds. *Ocean, ice and atmosphere: interactions at the Antarctic continental margin*. Washington, DC, American Geophysical Union, 83–99. (Antarctic Research Series 75.)
- Jacobs, S. S., H. H. Hellmer, C. S. M. Doake, A. Jenkins and R. M. Frolich. 1992. Melting of ice shelves and the mass balance of Antarctica. *J. Glaciol.*, **38**(130), 375–387.
- Jenkins, A. and A. Bombosch. 1995. Modeling the effects of frazil ice crystals on the dynamics and thermodynamics of Ice Shelf Water plumes. *J. Geophys. Res.*, **100**(C4), 6967–6981.
- Kottmeier, C. and L. Sellmann. 1996. Atmospheric and oceanic forcing of Weddell Sea ice motion. *J. Geophys. Res.*, **101**(C9), 20,809–20,824.
- Lewis, E. L. and R. G. Perkin. 1986. Ice pumps and their rates. *J. Geophys. Res.*, **91**(C10), 11,756–11,762.
- MacAyeal, D. R. 1984. Thermohaline circulation below the Ross Ice Shelf: a consequence of tidally induced vertical mixing and basal melting. *J. Geophys. Res.*, **89**(C1), 597–606.
- Manabe, S., M. J. Spelman and R. J. Stouffer. 1992. Transient responses of a coupled ocean–atmosphere model to gradual changes of atmospheric CO₂. Part II: Seasonal response. *J. Climate*, **5**(2), 105–126.
- Mellor, G. L. 1991. An equation of state for numerical models of oceans and estuaries. *J. Atmos. Oceanic Technol.*, **8**, 609–611.
- Nicholls, K. W. 1997. Predicted reduction in basal melt rates of an Antarctic ice shelf in a warmer climate. *Nature*, **388**(6641), 460–462.
- Schröder, M. and 9 others. 1997. Physikalische Ozeanographie, Nährstoffe und Tracer. *Ber. Polarforsch.*, **219**, 19–36.
- Vaughan, D. G. and C. S. M. Doake. 1996. Recent atmospheric warming and retreat of ice shelves on the Antarctic Peninsula. *Nature*, **379**(6563), 328–331.
- Vaughan, D. G. and 9 others. 1994. *Map of subglacial and seabed topography, Filchner/Ronne Schelfeis/Weddell Sea, Antarktis. 1: 2 000 000*. Frankfurt am Main, Institut für Angewandte Geodäsie.
- Williams, M. J. M., A. Jenkins and J. Determann. 1998. Physical controls on ocean circulation beneath ice shelves revealed by numerical models. In Jacobs, S. S. and R. F. Weiss, eds. *Ocean, ice and atmosphere: interactions at the Antarctic continental margin*. Washington, DC, American Geophysical Union, 287–301. (Antarctic Research Series 75.)
- Wingham, D. J. and 6 others. 1997. *ESAMCA (Exploitation of satellite imagery for the monitoring of climate-related change of Antarctic ice shelves) Project final report*. Holmbury St. Mary, U.K., Mullard Space Science Laboratory. (DGXII Environment Programme Phase II Contract EV5C-CT94-0483.)